

# Living with Genome Instability: Plant Responses to Telomere Dysfunction

Karel Riha,<sup>1</sup> Thomas D. McKnight,<sup>2</sup> Lawrence R. Griffing,<sup>2</sup>  
Dorothy E. Shippen<sup>1\*</sup>

Loss of telomere function in metazoans results in catastrophic damage to the genome, cell cycle arrest, and apoptosis. Here we show that the mustard weed *Arabidopsis thaliana* can survive up to 10 generations without telomerase. The last five generations of telomerase-deficient plants endured increasing levels of cytogenetic damage, which was correlated with developmental anomalies in both vegetative and reproductive organs. Mutants ultimately arrested at a terminal vegetative state harboring shoot meristems that were grossly enlarged, disorganized, and in some cases, dedifferentiated into a callusoid mass. Unexpectedly, late-generation mutants had an extended life-span and remained metabolically active. The differences in plant and animal responses to dysfunctional telomeres may reflect the more plastic nature of plant development and genome organization.

The integrity of eukaryotic genomes is derived in part from the architecture of telomeres, the nucleoprotein caps at chromosome ends. Telomeric DNA is usually maintained by telomerase, an enzyme whose RNA subunit serves as a template for reiterative addition of telomere repeat sequences by the reverse transcriptase subunit (TERT) (1). Mutations in telomerase cause telomere shortening, which ultimately limits cell proliferation capacity, because uncapped chromosome ends become indistinguishable from double-strand breaks and DNA damage checkpoints are activated. Cell cycle arrest, senescence, and apoptosis typically follow (2–4). After three generations, telomerase-deficient mice exhibit reduced fertility and progressive defects in highly proliferative organs (5–7). By the sixth generation, embryonic developmental defects (8) and collapse of the male reproductive system render mutants sterile (6). The terminal phenotype is delayed for two generations in mice deficient for both telomerase and p53, underscoring the essential role of cell cycle checkpoint proteins in sensing telomere dysfunction and limiting cell proliferation (9).

Plants display a more plastic pattern of development than animals and better tolerate extensive chromosomal rearrangements and ploidy changes (10). Here we report the consequences of telomere erosion in *Arabidopsis thaliana* by examining the fate of

plants through 10 generations of telomerase deficiency.

We generated four independent homozygous telomerase-deficient lines by selfing plants heterozygous for a transferred DNA (T-DNA) insertion into the single *AtTERT* gene (11). Detailed data are presented for one of these, line 69. We previously showed that line 69 plants were viable for at least two generations, although their telomeres shortened by ~500 base pairs (bp) per generation (12). Similarly, TRF (terminal restriction fragment) analysis performed on DNA extracted from generation two ( $G_2$ ),  $G_4$ ,  $G_6$ , and  $G_8$  mutant populations indicated that telomeres declined by 250 to 500 bp per generation (Fig. 1A). To investigate telomere dynamics in individual plants, we examined TRFs from individual  $G_1$  to  $G_8$  mutants. In all cases, heterogeneous TRFs in wild-type (WT) plants were replaced by discrete bands (Fig. 1B) that corresponded to individual chromosome ends (see below). Unexpectedly, TRFs did not decrease steadily. In five of nine mutants that we examined, a subset of TRFs increased relative to the previous generation (Fig. 1B, lanes  $G_4$  and  $G_5$ ) (13). Because line 69 was established from a single  $G_1$  plant, the increase in telomere length suggests that a telomerase-independent mechanism can extend telomeres in *Arabidopsis*.

Telomeres in three sibling  $G_1$  mutants were examined further with probes specific for individual telomeres. TRFs corresponding to the right arm of chromosome 2 and the left arm of chromosome 5 comigrated as sharp bands, consistent with a constant rate of telomere shortening due to the end replication problem (Fig. 1C). In contrast, TRF profiles for the left arm of chromosome 5 and some other undetermined telomere differed sub-

stantially among the siblings (Fig. 1C). These data imply that *Arabidopsis* telomeres are subject to stochastic telomere lengthening and shortening events, likely mediated by recombination and/or gene conversion. Because all plants in the population reached the terminal phenotype by the 10th generation (see below), permanent activation of an alternative telomere-lengthening mechanism (ALT), as previously described for telomerase-deficient yeast and cultured mammalian cells (14), must not have occurred in a cell destined to become germ line.

Telomere erosion leads to severe cytogenetic defects (15, 16) and delayed anaphase as a result of chromatid fusion (17). We determined the frequency of anaphase bridges in pistils as a gauge of genome stability. No bridges were observed in cells from the WT or  $G_{3-4}$  mutants (Fig. 2E). However, in  $G_5$  mutants, bridges were detected in 0.7% of the anaphases and by  $G_6$ , the number rose to 6% (Fig. 2E). The

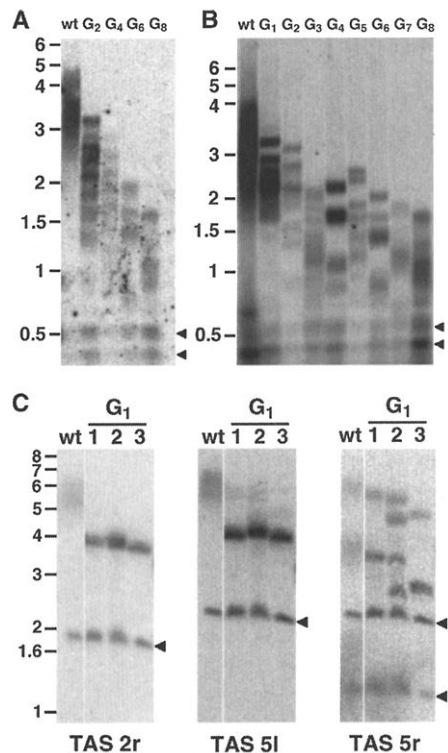


**Fig. 1.** Telomere dynamics in *AtTERT*<sup>-/-</sup> *Arabidopsis*. TRF analysis of DNA extracted from line 69 populations of ~100 sibling plants (A) or individual plants (B) derived from a sibling of their parent. Telomere lengths were determined by hybridization with a (T<sub>3</sub>AG<sub>3</sub>)<sub>4</sub> probe (12). (C) TRF analysis of individual chromosome arms in  $G_1$  sibling plants. Genomic DNAs were digested with Spe I, Hind III, and Pvu II and the membrane was sequentially hybridized with probes for telomere-associated sequences on the right arm of chromosome 2 (TAS 2r), left arm of chromosome 5 (TAS 5l), and right arm of chromosome 5 (TAS 5r). TAS 5r detects another unidentified telomere. Arrowheads indicate signals from interstitial sequences. Molecular size markers are indicated on the left (in kilobases).

<sup>1</sup>Department of Biochemistry and Biophysics, 2128 TAMU, Texas A&M University, College Station, TX 77843-2128, USA. <sup>2</sup>Department of Biology, Texas A&M University, College Station, TX 77843-3258, USA.

\*To whom correspondence should be addressed. E-mail: dshippen@tamu.edu

## REPORTS

frequency of bridges per anaphase increased in successive generations in direct proportion to the severity of the phenotype (Fig. 2, B, C, and E; see below). The onset of chromatid fusions in the mutants is consistent with uncapping of some chromosome ends (18). Anaphases with

five bridges (Fig. 2, C and E, class T) were observed in some late-generation flowers with severe developmental defects (see below), indicating that up to half of the chromosomes were fused. At this stage, bridges were detected in 44% of anaphases, and the average number of

fusions per anaphase was  $0.85 \pm 0.35$ . Some spreads had long, ribbonlike structures (Fig. 2D), which appeared to be giant, partially condensed linear DNA molecules resulting from end-to-end fusion of several chromosomes.

The mitotic index and the anaphase/meta-phase ratio in late-generation mutants was similar to those of WT plants (19), indicating that anaphase is not extended in response to telomere dysfunction in plants. The span of six generations between the initial appearance of anaphase bridges in  $G_5$  and total developmental arrest in  $G_{10}$  (see below) implies that telomerase-deficient plant cells, in contrast to their mammalian counterparts, continue cycling in the face of massive cytogenetic aberrations until total genomic catastrophe is reached.

Visually, *AtTERT*<sup>-/-</sup> plants were indistinguishable from WT through  $G_5$ , but from  $G_6$  onward, abnormalities became apparent, initially in vegetative organs and then in reproductive systems, worsening gradually in successive generations. Mutants were placed into four classes to reflect the onset of developmental defects and the progressive depletion of proliferative capacity: WT-like (no obvious phenotypic changes), I (mild defects in leaf morphology), II (moderate to severe defects in leaf morphology and shoot meristem structure and reduced germination efficiency), and T (terminal) (arrested in vegetative growth or unable to produce viable seeds) (Fig. 3). Although the fate of our four mutant lines was identical, the onset of defective phenotypes differed slightly (13), and one line reached the terminal phenotype in  $G_9$  (20).

The first defects appeared as rough sectors on leaves in a subset of  $G_{6-7}$  mutants (class I). In class II and terminal mutants, leaves were more severely affected. Leaf size was substantially reduced, many leaves were asymmetric and lobed (Fig. 4A), and in most leaves the entire surface was rough. The leaf lamina was thinner in rough sectors (Fig. 4B), with the number of mesophyll cells between epidermal layers reduced from four to five in WT to two to four in class I mutants. Although the epidermis was intact, cell size was increased by about fourfold relative to the WT (Fig. 4, C and D). Because plants can partially counterbalance defects in cell proliferation by varying cell size (21), we suspect that enlargement of epidermal cells compensates for the decreased proliferative capacity of cells with critically shortened telomeres.

The ultimate fate of terminal plants was arrest at the vegetative phase without an inflorescence bolt, or with a short bolt bearing sterile flowers (Fig. 3, A and B). Unexpectedly, both class II and terminal plants generated two to three times as many rosette leaves as WT plants (Fig. 4, E to G). Although this phenotype seems to be inconsistent with a

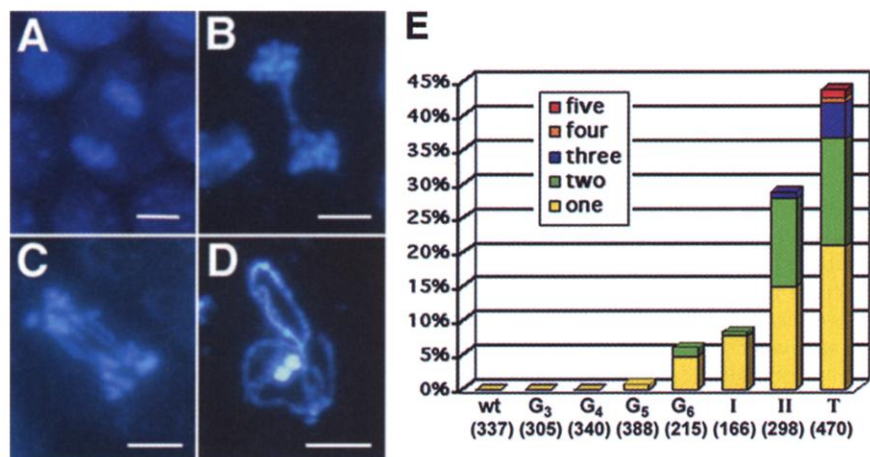


**Fig. 2.** End-to-end chromosome fusions in late-generation telomerase-deficient mutants. DAPI (4',6'-diamidino-2-phenylindole)-stained chromosome spreads were prepared from pistils as described (33). (A to D) Anaphase-staged chromosomes from WT (A) or mutants containing two (B) or five bridges (C) are shown along with a mitotic figure from a terminal plant (D). Bars, 3  $\mu$ m. (E) The frequency of anaphases with one to five bridges in late-generation mutants is shown. The total number of scored anaphases for each group is indicated in parentheses. The number of bridges may be underrepresented, because anaphases in which dicentric chromosomes were torn apart were not counted. I, II, and T represent classes of late-generation mutants with varying degrees of developmental abnormalities (see text for details).

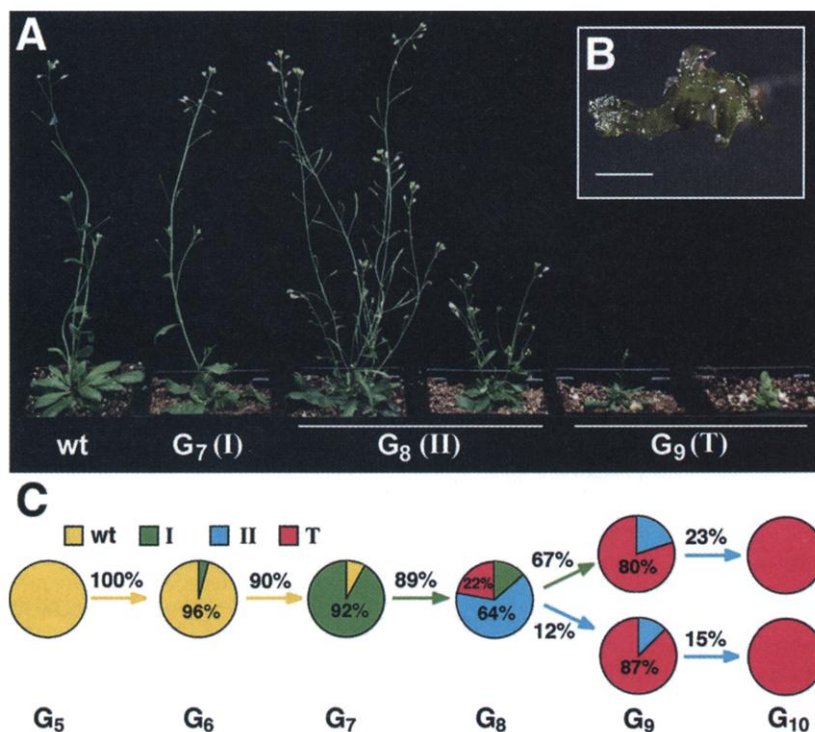


**Fig. 3.** Overview of phenotypes in telomerase-deficient *Arabidopsis*. (A) Placement of mutants into four classes: WT-like, I, II, and T (see text for details). (B) Terminal plant arrested early in vegetative development. Bar, 1 mm. (C) Distribution of phenotypes in  $G_5$  to  $G_{10}$  plants from line 69. Arrow colors denote plants used as parents for the next generation. Numbers above arrows indicate the efficiency of seed germination standardized to the germination efficiency of the WT.

## REPORTS

proliferative defect, it was accompanied by complex changes in the vegetative shoot apical meristem (SAM) (Fig. 4, H to J). Many late-generation mutants harbored a deformed, grossly enlarged SAM up to 500  $\mu\text{m}$  wide (Fig. 4, I and J), which is 10 to 20 times as large as that of the WT (Fig. 4H) (22). In some cases, fasciations and leaves initiated irregularly from the periphery (Fig. 4I), whereas in many terminal plants, the vegetative SAM was converted into a callusoid mass that stopped initiating leaves altogether (Fig. 4J).

Because the loss of telomere integrity limits cell proliferation capacity in other eukaryotes, net expansion and apparent dedifferentiation of SAM was unanticipated. Cell-autonomous and non-cell-autonomous models can be postulated to explain this phenomenon. The non-cell-autonomous model holds that rapidly dividing cells in the peripheral region deplete their proliferation capacity faster than quiescent stem cells, which disrupts intercellular communication essential for SAM integrity (23). Released from positional constraints, stem cells spend the remainder of their proliferative capacity in uncontrolled production of callus (Fig. 4J). The process could be gradual and dependent on the relative timing of telomere depletion because intermediate phenotypes, including plants with an enlarged SAM that initiated many deformed leaves (Fig. 4I), were commonly seen. Alternatively, a cell-autonomous model proposes that increased genomic instability in telomerase-deficient plants directly affects genes involved in SAM growth. Mutations or epigenetic effects in genes promoting either cell differentiation or stem cell maintenance (24, 25) could at least partially explain some of the mutant phenotypes. The increased rate of tumor formation in telomerase-deficient mice harboring defective DNA damage checkpoint mechanisms has been interpreted in the context of a similar cell-autonomous model (9, 26).

As expected, defects in reproduction were associated with telomerase-deficient plants, although the onset was slightly delayed relative to vegetative defects. Flower morphology in class I plants was generally unaffected (13), but some anthers were smaller and contained fewer pollen grains. This phenotype was exacerbated in later generations and terminal plants, if able to produce generative organs, harbored undeveloped anthers with few if any pollen grains (Fig. 4K). Whereas WT siliques typically contain ~50 seeds, seed yield in siliques from class I mutants was reduced by 10 to 50%, and from class II mutants, by 50 to 100%. Furthermore, in late-generation mutants, undeveloped ovules were commonly observed interspersed among normal developing seeds, indicating sporadic failure in ovule development or insufficient pollen for fertilization (Fig. 4L). Germination efficiency steadily declined

from  $G_7$  onward, and most of the seeds in  $G_9$  were not viable (Fig. 3C).

In contrast to animals, plants do not separate germ line from soma in early embryogenesis. Instead, gametes are derived from SAM after the development of vegetative organs. The ability of telomerase-deficient plants to produce viable seeds for four generations ( $G_6$  to  $G_9$ ) despite worsening defects in vegetative growth is exceptional. Two models could explain sustained fertility. First, gametes may be derived from a pool of cells that divide very slowly during vegetative growth, such as cells from the central zone of SAM (22). Alternatively, genome integrity may be actively monitored during gametophyte development so that only those cells meeting some minimal criteria are selected to form the germ line (10). Either or both of these models could account for the unusually

long lag between the onset of the first developmental defects ( $G_6$ ) and the expression of terminal phenotypes in all plants in a population ( $G_{10}$ ) (Fig. 3C).

Programmed cell death is frequently associated with telomere dysfunction in metazoans (6, 9, 27, 28); however, this may not be the case with plants, in which no functional homolog of p53 has been identified (29). Furthermore, although proliferative defects were observed in all stages of development, we could not detect a classic apoptotic DNA fragmentation ladder (30) or evidence for chlorophyll degradation (31) in leaves of the most severely affected mutants. Finally, class II and terminal plants had a substantially longer life-span than their WT counterparts. Whereas leaves in WT *Arabidopsis* become senescent during seed maturation (31), the leaves of telomerase-deficient mutants, de-

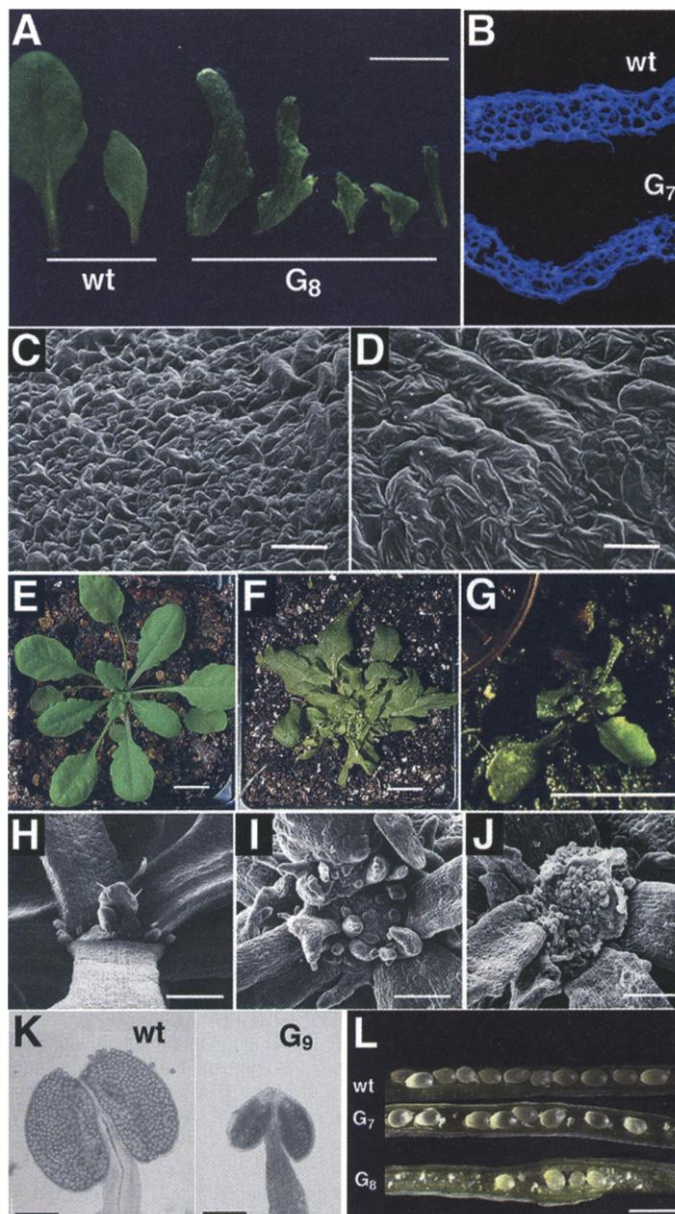


**Fig. 4.** Developmental defects in telomerase-deficient plants. (A to D) Leaf morphology. (A) Rosette and cauline leaves from WT (left to right), and two rosette and three cauline leaves from  $G_8$  (class II). Bar, 10 mm. (B) Transverse section of WT lamina and rough sectors of a class I leaf. Cell walls were stained with Calcofluor (Molecular Probes, Eugene, Oregon) (34). Dorsal surfaces of size-matched WT (C) and class II (D) leaves from  $G_8$  viewed by scanning electron microscopy (35). Bars, 50  $\mu\text{m}$ . (E to J) SAM architecture. WT (E), class II (F), and terminal plants arrested early in development (G). Bars, 1 cm. Scanning electron micrographs of SAM in WT (H), fasciated SAM in class II (I), and callusoid SAM in terminal mutants arrested in vegetative growth (J). Bars, 300  $\mu\text{m}$ . (K and L) Reproductive defects in telomerase-deficient plants. Anthers (K) from WT (left) and terminal  $G_9$  plants (right) (36). Bars, 200  $\mu\text{m}$ . Viability of pollen from WT and late-generation plants was similar, as gauged by fluorescein diacetate staining (13). Siliques (L) from WT, class I ( $G_7$ ), and class II ( $G_8$ ) mutants. Bars, 1 mm.

spite their severely impaired growth, remained green and metabolically active for months, long after the WT died (32). These observations, in conjunction with the severe cytogenetic anomalies borne by late-generation mutants, imply that aspects of the primary cellular response to telomere dysfunction are unique to plants and may reflect the unusual plasticity of their development and genome organization. Nevertheless, an efficient telomere maintenance mechanism is crucial for indefinite cell proliferation and hence, telomerase-deficient *Arabidopsis* may offer new insight into pathways coordinating DNA checkpoint mechanisms and DNA repair.

References and Notes

1. V. Lundblad, *Proc. Natl. Acad. Sci. U.S.A.* **95**, 8415 (1998).
2. P. M. Lansdorpe, *Mech. Ageing Dev.* **118**, 23 (2000).
3. R. Oulton, L. Harrington, *Curr. Opin. Oncol.* **12**, 74 (2000).
4. V. Lundblad, *Mutat. Res.* **451**, 227 (2000).
5. M. A. Blasco et al., *Cell* **91**, 25 (1997).
6. H.-W. Lee et al. *Nature* **392**, 569 (1998).
7. L. Rudolph et al. *Cell* **96**, 729 (1999).
8. E. Herrera, E. Samper, M. A. Blasco, *EMBO J.* **18**, 1172 (1999).
9. L. Chin et al. *Cell* **97**, 527 (1999).
10. V. Walbot, *Trends Plant Sci.* **1**, 27 (1996).
11. G<sub>1</sub> mutants were obtained by selfing plants heterozygous for a T-DNA insertion in *AtTERT* (12). Five homozygous lines were generated from the progeny of individual G<sub>1</sub> plants, one from the WT (line 71) and four from mutant G<sub>1</sub> plants (lines 16, 20, 69, and 96). Individual lines were propagated through successive generations by selfing. Seeds from several plants within a single line were pooled in each generation until G<sub>6</sub>. From G<sub>6</sub> onward, individual plants were examined. Plants were grown in continuous light at 21°C in an environmental growth chamber.
12. M. S. Fitzgerald et al., *Proc. Natl. Acad. Sci. U.S.A.* **96**, 14813 (1999).
13. K. Riha, D. E. Shippen, unpublished data.
14. A. Kass-Eisler, C. W. Greider, *Trends Biochem. Sci.* **25**, 200 (2000).
15. M. P. Hande, E. Samper, P. Lansdorpe, M. A. Blasco, *J. Cell Biol.* **144**, 589 (1999).
16. S. E. Artandi et al., *Nature* **406**, 641 (2000).
17. K. E. Kirk, B. P. Harmon, I. K. Reichardt, J. W. Sedat, E. H. Blackburn, *Science* **275**, 1478 (1997).
18. Telomeres range in size from 2 to 4.5 kb in WT cells. In G<sub>6</sub> mutants, the longest telomeres were 2 kb; the shortest were only a few hundred base pairs (13).
19. The proportion of cells in mitosis [mitotic index (MI)] and the anaphase/metaphase ratio (A/M) were calculated for pistils from WT and class II/terminal plants. MI<sub>WT</sub> = 1.94 ± 0.32 (n = 6), MI<sub>mutant</sub> = 2.4 ± 0.33 (n = 7), A/M<sub>WT</sub> = 0.85 ± 0.10 (n = 4), A/M<sub>mutant</sub> = 0.83 ± 0.06 (n = 5).
20. Supplementary data are available on Science Online at [www.sciencemag.org/cgi/content/full/291/5509/1797/DC1](http://www.sciencemag.org/cgi/content/full/291/5509/1797/DC1).
21. S. E. Clark, J. W. Schiefelbein, *Trends Cell Biol.* **7**, 454 (1997).
22. P. Laufs, O. Grandjean, C. Jonak, K. Kieu, J. Traas, *Plant Cell* **10**, 1375 (1998).
23. J. C. Fletcher, E. M. Meyerowitz, *Curr. Opin. Plant Biol.* **3**, 23 (2000).
24. E. M. Meyerowitz, *Cell* **88**, 299 (1997).
25. T. Laux, K. F. Mayer, *Semin. Cell Dev. Biol.* **9**, 195 (1998).
26. T. de Lange, T. Jacks, *Cell* **98**, 273 (1999).
27. J. Karlseder, D. Broccoli, Y. Dai, S. Hardy, T. de Lange, *Science* **283**, 1321 (1999).
28. K. Ahmad, K. G. Golic, *Genetics* **151**, 1041 (1999).
29. S. J. Klosterman, J. J. Choi, L. A. Hadwiger, *Physiol. Mol. Plant Pathol.* **56**, 197 (2000).
30. To investigate whether leaf cells respond to telomere depletion by apoptosis, we extracted genomic DNA from leaves of WT, G<sub>6</sub>, and G<sub>9</sub> mutants using a

- DNeasy plant kit (Qiagen). DNA from four WT and six terminal plants was subjected to electrophoresis in a 1.5% agarose gel, transferred onto a Nylon membrane (MSI, Westborough, MA), and hybridized with radioactively labeled total genomic DNA. No difference in the DNA profiles was observed.
31. A. B. Blecker, *Curr. Opin. Plant Biol.* **1**, 73 (1998).
32. WT plants grown at short day (8 hours of light) produced seeds after 10 weeks. Seed production was accompanied by senescence, and death occurred by the fourth month. In contrast, class II and some terminal mutants remained in the vegetative stage much longer and started to flower after 6 months.
33. J. S. Heslop-Harrison, in *Arabidopsis Protocols*, J. Martinez-Zapater, J. Salinas, Eds. (Humana, Totowa, NJ, 1998), vol. 82, p. 119.

34. J. Hughes, M. E. McCully, *Stain Technol.* **50**, 319 (1975).
35. V. Vasil, I. K. Vasil, in *Cell Culture and Somatic Cell Genetics of Plants* (Academic Press, London, 1984), vol. 1, p. 738.
36. Anthers were fixed in ethanol/acetic acid solution (3:1) and gently squashed in a drop of 60% acetic acid with a cover slip. Slides were observed by light microscopy.
37. We thank J. Chen, A. Pepper, P. Lansdorpe, C. Price, and B. Vyskot for insightful comments on the manuscript. Funded by NSF grant MCB982499 (T.D.M. and D.E.S.) and a NATO-NSF postdoctoral fellowship (K.R.).

2 November 2000; accepted 22 January 2001

## Role of the Sphingosine-1-Phosphate Receptor EDG-1 in PDGF-Induced Cell Motility

John P. Hobson,<sup>1\*</sup> Hans M. Rosenfeldt,<sup>1\*</sup> Larry S. Barak,<sup>2</sup>  
Ana Olivera,<sup>1</sup> Samantha Poulton,<sup>1</sup> Marc G. Caron,<sup>2</sup>  
Sheldon Milstien,<sup>3</sup> Sarah Spiegel<sup>1†</sup>

EDG-1 is a heterotrimeric guanine nucleotide binding protein-coupled receptor (GPCR) for sphingosine-1-phosphate (SPP). Cell migration toward platelet-derived growth factor (PDGF), which stimulates sphingosine kinase and increases intracellular SPP, was dependent on expression of EDG-1. Deletion of *edg-1* or inhibition of sphingosine kinase suppressed chemotaxis toward PDGF and also activation of the small guanosine triphosphatase Rac, which is essential for protrusion of lamellipodia and forward movement. Moreover, PDGF activated EDG-1, as measured by translocation of β-arrestin and phosphorylation of EDG-1. Our results reveal a role for receptor cross-communication in which activation of a GPCR by a receptor tyrosine kinase is critical for cell motility.

Interest in SPP has accelerated recently with the discovery that it is the extracellular ligand for EDG-1, EDG-3, EDG-5, EDG-6, and EDG-8 (1). Although the biological functions of these GPCRs have not been completely elucidated, EDG-1 is implicated in cell migration, angiogenesis, and vascular maturation (2–4). Disruption of the *edg-1* gene by homologous recombination in mice resulted in massive intra-embryonic hemorrhaging and intrauterine death caused by incomplete vascular maturation resulting from a failure of mural cells—vascular smooth muscle cells and pericytes—to migrate to arteries and capillaries and to reinforce them

properly (4). Disruption of the *PDGF-BB* or *PDGFR-β* genes in mice resulted in a similar lethal phenotype (5, 6). Because in many different cell types, PDGF stimulates sphingosine kinase, leading to an accumulation of intracellular SPP (1, 7), we speculated that interplay between PDGF and SPP–EDG-1 signals might be required for cell migratory responses. In this study, we found that activation of EDG-1 by the PDGFR plays a crucial role in regulating cell motility. The results reveal a new paradigm for communication between tyrosine kinase receptors and GPCRs.

Human embryonic kidney (HEK) 293 cells, which only express EDG-3 and EDG-5, did not migrate toward SPP unless EDG-1 was expressed (2). EDG-1 overexpression also stimulated migration of HEK 293 cells toward PDGF-BB (Fig. 1A), whereas migratory responses to serum and fibronectin were unaffected (Fig. 1A). Conversely, migration of mouse embryonic fibroblasts (MEFs), which express transcripts for EDG-1, EDG-3, and EDG-5, but not EDG-6 or EDG-8 (4), toward PDGF-BB was reduced when *edg-1* was deleted (Fig. 1B).

<sup>1</sup>Department of Biochemistry and Molecular Biology, Georgetown University Medical Center, Washington, DC 20007, USA. <sup>2</sup>Howard Hughes Medical Institute Laboratories and Department of Cell Biology, Duke University Medical Center, Durham, NC 27710, USA. <sup>3</sup>Laboratory of Cellular and Molecular Regulation, National Institute of Mental Health, Bethesda, MD 20892, USA

\*These authors contributed equally to this report.  
†To whom correspondence should be addressed. E-mail: [spiegel@bc.georgetown.edu](mailto:spiegel@bc.georgetown.edu)